THE GERONTOLOGICAL SOCIETY OF AMERICA®

Journals of Gerontology: Medical Sciences
cite as: *J Gerontol A Biol Sci Med Sci*, 2020, Vol. 75, No. 9, 1744–1753
doi:10.1093/gerona/glaa001
Advance Access publication January 7, 2020

OXFORD

Research Article

Skeletal Muscle Energetics and Mitochondrial Function Are Impaired Following 10 Days of Bed Rest in Older Adults

Robert A. Standley, PhD,[1] Giovanna Distefano, PhD,[1] Michelle B. Trevino, PhD,[2] Emily Chen, PhD,[3] Niven R. Narain, PhD,[3] Bennett Greenwood, PhD,[3] Gramoz Kondakci, PhD,[3] Vladimir V. Tolstikov, PhD,[3] Michael A. Kiebish, PhD,[3] Gongxin Yu, PhD,[1] Feng Qi, PhD,[2] Daniel P. Kelly, MD,[2,4] Rick B. Vega, PhD,[1,2] Paul M. Coen, PhD,[1,*] and Bret H Goodpaster, PhD[1,2]

[1]AdventHealth Translational Research Institute, Orlando, Florida. [2]Center for Metabolic Origins of Disease, Sanford Burnham Prebys Medical Discovery Institute, Orlando, Florida. [3]BERG LLC, Framingham, Massachusetts. [4]Penn Cardiovascular Institute, Perelman School of Medicine at the University of Pennsylvania, Philadelphia.

*Address correspondence to: Paul M. Coen, PhD, AdventHealth Translational Research Institute for Metabolism and Diabetes, 301 E. Princeton St., Orlando, FL 32814. E-mail: paul.coen@AdventHealth.com

Received: August 1, 2019; Editorial Decision Date: December 28, 2019

Decision Editor: Jay Magaziner, MSHyg, PhD

Abstract

Background: Older adults exposed to periods of inactivity during hospitalization, illness, or injury lose muscle mass and strength. This, in turn, predisposes poor recovery of physical function upon reambulation and represents a significant health risk for older adults. Bed rest (BR) results in altered skeletal muscle fuel metabolism and loss of oxidative capacity that have recently been linked to the muscle atrophy program. Our primary objective was to explore the effects of BR on mitochondrial energetics in muscle from older adults. A secondary objective was to examine the effect of β-hydroxy-β-methylbuturate (HMB) supplementation on mitochondrial energetics.

Methods: We studied 20 older adults before and after a 10-day BR intervention, who consumed a complete oral nutritional supplement (ONS) with HMB (3.0 g/d HMB, n = 11) or without HMB (CON, n = 9). Percutaneous biopsies of the *vastus lateralis* were obtained to determine mitochondrial respiration and H_2O_2 emission in permeabilized muscle fibers along with markers of content. RNA sequencing and lipidomics analyses were also conducted.

Results: We found a significant up-regulation of collagen synthesis and down-regulation of ribosome, oxidative metabolism and mitochondrial gene transcripts following BR in the CON group. Alterations to these gene transcripts were significantly blunted in the HMB group. Mitochondrial respiration and markers of content were both reduced and H_2O_2 emission was elevated in both groups following BR.

Conclusions: In summary, 10 days of BR in older adults causes a significant deterioration in mitochondrial energetics, while transcriptomic profiling revealed that some of these negative effects may be attenuated by an ONS containing HMB.

Keywords: Mitochondria, Transcriptomics, Bed rest, Aging, HMB

Skeletal muscle atrophy is a clinically significant problem that occurs during disuse or immobilization due to hospitalization, illness, and injury, and leads to a loss of muscle strength and physical function (1). This is a particular public health problem for older adults who comprise the majority of hospital patients in the United States (2) and who may lose more muscle mass during bed rest (BR) (3). Older adults do not adequately recover following BR without adequate rehabilitation (4), which likely contributes to their reduced functional status and ambulation upon discharge (5), a loss of independence, nursing home placement (6), and an increased risk for falls and fractures (7).

Muscle mass is maintained by a balance between protein synthesis and degradation. Recent evidence from preclinical models indicates a close link between mitochondrial energetics and control of muscle mass. Mitochondrial oxidative stress has been reported to stimulate muscle protein breakdown by activating lysosome-autophagy

and proteasome systems (8) and energetic stress due to reduced ATP production, which may also activate the adenosine monophosphate-activated protein kinase (AMPK)-FoxO3 pathways leading to increased protein degradation (9). Promoting mitochondrial biogenesis by overexpression of PGC-1α protects muscle mass from acute atrophy due to immobilization or disuse (10). Considered together, this evidence suggests a central role for mitochondrial energetics in regulating muscle mass.

Derangements in metabolism that contribute to muscle atrophy include skeletal muscle insulin resistance (11), decreased fatty acid oxidation and a shift to glucose oxidation (12), intramyocellular lipid accumulation (13), and impaired protein synthesis (14). While mitochondria have been implicated in the etiology of these metabolic dysfunctions in the context of aging per se (15), the role of mitochondria in human muscle disuse atrophy and loss of function is poorly understood, particularly in older adults. Recently, Dirks et al. found that younger men had a reduction in mitochondrial OXPHOS content after 10 days of BR; however, markers of oxidative stress were unchanged (16). Kenny et al. showed that reductions in muscle mitochondrial respiration occur concomitantly with insulin resistance and loss of muscle mass during BR in healthy young men (17). Further evidence linking mitochondrial energetics to muscle mass and physical function could be critical to help determine whether mitochondria are viable therapeutic targets for muscle health of older adults during and following disuse.

The primary objective of this study was to examine changes in skeletal muscle mitochondrial energetics during a period of disuse in older men and women. Therapeutic strategies to preserve muscle health during inactivity and facilitate effective recovery upon reambulation have included nutritional supplementation with branched chain amino acids (BCAA), and β-hydroxy-β-methylbuturate (HMB). We have previously shown that HMB supplementation had a positive impact on OXPHOS content in older adults following BR (18). Our findings are congruent with preclinical studies that highlight a potential impact of HMB to promote mitochondria and oxidative metabolism beyond its known impact on protein metabolism (19,20). Our goal here was to further explore the impact of HMB on mitochondria and oxidative metabolism. A secondary objective was to take a comprehensive approach to examine the effect of a complete oral nutritional supplement with and without HMB on skeletal muscle mitochondria content, function, and gene regulatory networks related to mitochondrial biogenesis and energetics. We combined both targeted and unbiased approaches to examine interrogate skeletal muscle transcriptome and lipidome, skeletal muscle mitochondrial content, and function in healthy older adults in response to disuse while consuming a complete oral nutritional supplement.

Methods

Study Design

The study design was a prospective, randomized, double-blinded, placebo-controlled trial. Eligible subjects were randomized into one of the two groups, consuming twice daily complete oral nutritional supplementation (ONS); either with 1.5 g calcium (Ca)-HMB (HMB) or without HMB (Control; CON). The total dose of HMB was 3 g/d. The randomization was stratified by gender and age (60–69 years, 70–79 years). The composition of the control tetrapak was identical to the HMB tetrapak with the exclusion of the Ca-HMB and both supplements were packaged indistinguishably by Abbott Nutrition. Treatment with ONS was initiated 5 days prior to BR and continued until the end of BR. For diet stabilization over the 5 days Pre-BR Period, subjects were fed a control diet providing the RDA for protein intake (0.8 g protein/kg body weight/d). Total caloric needs were estimated using the Harris-Benedict equation for resting energy expenditure with an activity factor of 1.375 for the ambulatory Pre-BR and 1.1 for the BR periods. The remaining macronutrients were distributed according to national dietary guidelines.

Following the 5 days diet stabilization (ambulatory period), subjects remained in BR for 10 days. While confined to BR, preventative measures were taken to detect and prevent deep vein thrombosis (DVT) including passive range of motion exercises, the use of Thrombo-Embolism Deterrent hose (TED), and Sequential Compression Device (SCD) throughout BR. If DVT was suspected, subjects received a clinical exam and a bilateral lower extremity venous ultrasound.

Subjects

A total of 21 subjects were randomized to HMB or CON and 1 subject (CON group) dropped from the study prior to BR. The study was conducted at the AdventHealth Translational Research Institute for Metabolism and Diabetes (TRI-MD) and approved by the Institutional Review Board of AdventHealth. All study procedures, risks, and benefits were explained to the subjects before giving written consent to participate. The subjects recruited for this investigation were a subset of subjects who were part of a larger clinical trial (NCT#02090387).

The following inclusion criteria were verified at screening: male or female ≥60 to ≤79 years of age; body mass index (BMI) ≥20 but ≤35 kg/m^2; ambulatory with a Short Physical Performance Battery (SPPB) score of ≥9; LDL cholesterol ≤155 mg/dL, total cholesterol ≤250 mg/dL, and total triglycerides ≤250 mg/dL, with or without statin use or other blood lipid lowering agents; an ankle brachial index between 1 and 1.4 as defined by the American Heart Association Task Force on Practice Guidelines; a physical activity score between 7.5 and 17.7 metabolic equivalents (METs) or above by the CHAMPS Physical Activity Questionnaire for older adults; and handgrip strength ≥29 kg for males and ≥18.5 kg for females. Exclusion criteria ruled out subjects who have been diagnosed with Type I or Type II diabetes mellitus; taking drugs known to impact glucose metabolism; fasting blood glucose >115 mg/dL without use of medications; undergone recent major surgery; has history of ulcers, DVT, or other hypercoagulation disorders, significant cardiovascular events or congestive heart failure, neurological or other psychiatric disorders, and allergy to any of the ingredients in the study products; had active malignancy (except basal of squamous cell skin carcinoma or carcinoma in situ of the uterine cervix); estimated glomerular filtration rate <50 mL/min/1.73 m^2; current impaired liver function or hepatic enzymes ≥2.5 times normal limit; untreated hypo- or hyper-thyroidism; had a chronic, contagious infectious disease; chronic or acute gastrointestinal (GI) disease; an amputee; and actively pursuing weight loss. Potential subjects were also excluded if they were taking any medications known to affect protein metabolism, and could not refrain from taking long chain n-3 polyunsaturated fatty acids, or vitamin D above the established Acceptable Macronutrient Distribution Range.

Skeletal Muscle Biopsy

Subjects underwent a muscle biopsy of the *m. vastus lateralis* before and on the last day of BR. The biopsy sample was taken

10–15 cm above the knee under local anesthesia (2% buffered lidocaine) with a 5-mm Bergstrom needle with suction, as described previously (21). Approximately 10–15 mg of muscle was placed in biopsy-preserving solution (BIOPS media) for fresh tissue analysis of mitochondrial respiration and H_2O_2 emission. A separate portion of the sample was prepared for immunohistochemistry, and the remaining muscle sample was immediately frozen in liquid nitrogen (–190°C) until analysis.

High-Resolution Respirometry and ROS Emission

Permeabilized fiber bundles (1–3 mg) were prepared immediately following the muscle biopsy, as previously described (22). Briefly, individual myofibers were gently teased apart in a petri dish containing ice-cold BIOPS media. The fiber bundles were then permeabilized in saponin (2 mL of 50 µg/mL) for 20 minutes and washed twice (10 minutes each) in Buffer Z (105 mM K-MES, 30 mM KCl, 10 mM KH_2PO_4, 5 mM $MgCl_2$-$6H_2O$, 5 mg/mL BSA, 1 mM EGTA, pH 7.4 with KOH). Mitochondrial respiration was evaluated by high-resolution respirometry (Oxygraph-2k, Oroboros Instruments, Innsbruck, Austria). Measurements were performed at 37°C, in the range of 200–400 nmol O_2/mL, in duplicate using Buffer Z with blebbistatin (25 µm). The assay protocol was as follows: Complex I supported LEAK (L_I) respiration was determined through the addition of glutamate (5 mM) and malate (2 mM). ADP (4 mM) was added to elicit complex I-supported OXPHOS (P_I) respiration. Succinate (10 mM) was added to elicit complex I&II -supported OXPHOS (P_{I+II}). Cytochrome c (10 µM) was added to assess the integrity of the outer mitochondrial membrane. Finally, FCCP (1 µM steps) was added to determine maximal complex I&II-supported electron transfer system capacity (E) or maximal uncoupled respiration.

Measurement of H_2O_2 emission by mitochondria was measured in permeabilized muscle fiber bundles by real-time monitoring of amplex red oxidation using a SPEX Fluoromax 4 (Horiba Scientific, Edison, NJ) spectrofluorometer with temperature control (37°C) and magnetic stirring as preciously described (23). Briefly, the assay was run with buffer Z containing 5,000U/mL CuZn-SOD, 25 µM blebbistatin, 50 µM amplex ultra-red, and 6U/mL horseradish peroxidase in the presence of 10 µg/mL oligmycin, 10 mM glutmate, 2 mM malate, and 10 mM succinate. The rate of emission of H_2O_2 (pmol) was calculated from previously established fluorescence intensity standard curves with known concentrations of H_2O_2, after correcting for the rate of change in background fluorescence. The rate of H_2O_2 emission was expressed as pmol/min/mg dry weight of fiber bundle.

Immunohistochemistry

Histochemical analyses were performed on serial sections using methods previously described (24). Briefly, muscle was placed vertically in mounting medium on cork and frozen in isopentane cooled with liquid nitrogen until thoroughly frozen. Biopsy samples were sectioned (10 µm) using a cryotome and fixed prior staining. Sections were incubated in primary antibody cocktail at 4°C overnight (in 10% goat serum), which includes BA-F8 (type I): IgG2b (1:50); 6H1 (type IIx): IgM (1:50); and sc-71 (type IIa): IgG1 (1:50). All antibodies were obtained from the University of Iowa Hybridoma Bank. Following primary antibody incubation, slides were incubated in secondary antibody cocktail consisting of DyLight 405 (IgG2b) goat anti-mouse (1:500), Alexa Fluor 555 (IgM) goat anti-mouse (1:500), and Alexa Fluor 488 (IgG1) goat anti-mouse (1:500). In addition, Alexa Fluor 647-conjugated wheat germ agglutinin (WGA) (50 mg/mL for 30 minutes in dark at RT) was used to stain glycoconjugates (N-acetylglucosamine and N-acetylneuraminic acid) residues. Digital images (4× magnification) of one section per skeletal muscle biopsy were captured using a Nikon eclipse Ti microscope (Nikon Technologies, California) and image analysis was performed using NIS elements software 4.20.01.

Western Blot

Muscle homogenates were prepared as previously described (18,25). Protein was loaded on a 4%–20% gel (Bio-Rad, Mini-PROTEAN TGX Precast Gel) and transferred onto a nitrocellulose membrane overnight at 30 mA at 4°C. Membranes were blocked with 5% non-fat milk for 1 hour and then incubated with primary antibody overnight at 4°C (anti-polyubiquitin, Enzo Life Sciences, Farmingdale, NY, 1:1,000; OXPHOS, MitoSciences, Eugene, OR; α-tubulin, Cell Signaling, Danvers, MA). Membranes were then incubated with secondary antibody for 1 hour (IRDye 800CW anti-Rabbit IgG and IRDye 680RD anti-Mouse IgG; Li-Cor Biosciences, Lincoln, NE). Protein bands were visualized as described above. The amount of poly-ub proteins was normalized to tubulin. Gel-to-gel variation was controlled for by using a standardized sample on each gel.

Real-Time Quantitative-PCR

Total RNA was isolated from ~20 to 30 mg of skeletal muscle tissue using the RNeasy Fibrous Tissue kit (Qiagen, Valencia, CA) and transcribed to cDNA using the AffinityScript qPCR cDNA synthesis kit (Agilent Technologies, Santa Clara, CA). Specific oligonucleotide primers for target gene sequences are listed in Supplementary Table 1. Gene expression was measured with the Roche LightCycler 480 Real-time PCR system (Roche, Indianapolis, IN). Arbitrary units of target mRNA were corrected to the expression of expression of 36b4 (*Rplp0*).

RNA Sequencing and Informatics

The quality of total RNA was assessed by the Agilent Bioanalyzer Nano chip (Agilent Technologies). One microgram of total RNA was used as starting material to construct RNA Seq library using Illumina's Truseq Stranded total RNA Library preparation kit. First, the total RNA was Ribo depleted to remove rRNA from total RNA. The remaining non-rRNA was fragmented into small pieces using divalent cations under elevated temperature. Following fragmentation, the first-strand cDNA was synthesized using random primers and followed by second strand synthesis using DNA Polymerase I. The cDNA was then ligated with index adapters for each sample followed by purification and then enriched with PCR to create the final library. The quality and quantity of the libraries were detected by Agilent Bioanalyzer and Kapa Biosystems qPCR. Multiplexed libraries are pooled and single-end 50-bp sequencing was performed on one flow-cell of an Illumina Hiseq 2500. Mapped reads were filtered based on the mapping quality. The overall mapping rates were about 90%. mRNA quantification and normalization were done using Partek Genomics Suite 6.6, annotation database using RefSeq Transcript 77 July 2016. R package DeSeq (http://bioconductor.org/packages/release/bioc/html/DESeq.html) was used to analyze the differential expression of mRNAs. Heat maps were created with Morpheus (Broad Institute). The database for annotation, visualization, and integrated discovery (DAVID v6.8) was used for gene ontology (GO) annotation. Upstream regulator analysis was

performed with Ingenuity Pathway Analysis (Qiagen). The gene expression data discussed in this publication have been deposited in NCBI's Gene Expression Omnibus and are accessible through GEO Series accession number GSE130722 (https://www.ncbi.nlm.nih.gov/geo/query/acc.cgi?acc=GSE130722).

Lipidomics

Muscle tissue was thawed in 10 times diluted PBS and homogenized in Omni bead tubes with 2.8-mm ceramic beads in the Omni Bead Ruptor 24 with Cryo Cooling Unit (Omni International) at 4°C for 2 minutes. Protein concentration was determined by the bicinchoninic acid assay. One milligram of protein from each sample was aliquoted, and a cocktail of deuterium-labeled and odd chain phospholipid standards from diverse lipid classes was added. Standards were chosen so that they represented each lipid class and were at designated concentrations chosen to provide the most accurate quantitation and dynamic range for each lipid species. Four milliliters of chloroform:methanol (1:1, by volume) were added to each sample, and lipidomic extractions were performed as previously described (26). Lipid extraction was automated using a customized sequence on a Hamilton Robotics STARlet system (Hamilton). Lipid extracts were dried under nitrogen and reconstituted in chloroform:methanol (1:1, by volume). Samples were flushed with nitrogen and stored at –20°C.

The concentrated sample was diluted 50× in isopropanol:methanol:acetonitrile:H_2O (3:3:3:1, by volume) with 2 mM ammonium acetate. The delivery of the solution to the SCIEX TripleTOF 5600+ (Sciex, Framingham, MA) was carried out using an Ekspert MicroLC 200 system with a flow rate at 6 µL/min on a customized loop. The parameters of the mass spectrometer were optimized, and the samples were analyzed automatically using a data independent analysis strategy, allowing for MS/MSALL high-resolution and high-mass accuracy (27).

Statistical Analysis

All data are reported as means ± standard error unless otherwise stated. Statistical analysis was performed using SAS (SAS, Cary, NC) and Graphpad Prism v6 (GraphPad Software, Inc, La Jolla, CA). The differences between groups were examined using a two-way analysis of variance (Group × Time) with Bonferroni multiple comparisons when appropriate. Skeletal muscle fiber cross-sectional area was analyzed using a two-way analysis of covariance controlling for baseline differences between the groups. Significance was set at $p < .05$.

Results

Subject Characteristics

Subject characteristics are presented in Table 1. The HMB group had more females compared to the CON group, which led to group differences in height and BMI (Table 1). Due to these baseline differences, we used gender and BMI as covariates in the statistical models when examining changes in muscle fiber cross-sectional area (CSA) following BR.

Markers of Skeletal Muscle Atrophy

Skeletal muscle CSA determined by immunohistology are presented in Figure 1A and B. Type I and type IIa skeletal muscle CSA (Figure 1A) and frequency histograms (Figure 1B) indicate a reduction in type IIa muscle fiber CSA following BR (Time Effect: $p = .03$). There were no significant changes in type I muscle fiber CSA following BR. Representative images of immunostained muscle cross sections are presented in Supplementary Figure 1. We then measured the levels of gene transcripts and proteins that govern the skeletal muscle atrophy program. Gene expression levels of atrogin-1 (*FBXO32*) tended to increase following BR (Time Effect: $p = .069$). There were no significant changes in the level of MuRF1 (*TRIM63*) expression (Figure 1C). Total poly-ubiquinated proteins tended to increase (Group Effect: $p = .078$, Interaction: 0.10) following BR in the HMB group (Figure 1D).

Skeletal Muscle Transcriptomics

RNA sequencing (RNA-seq) was next performed to determine the transcriptomic changes that occur during BR. Principal component analysis demonstrates a separation in the control and HMB groups, as well as a significant change for both groups following BR (Figure 2A). GO enrichment analysis demonstrated a reduction in transcripts associated with the ribosome consistent with decreased protein synthesis known to occur during disuse atrophy (Supplementary Figures 2 and 3). In addition, GO terms for fibrosis-related processes such as extracellular matrix and collagen were enriched when up-regulated transcripts were used (Supplementary Figures 2 and 3). Examination of transcripts in both ribosome and collagen trimer pathways confirmed these findings (Figure 2B and C, Supplementary Tables 2 and 3). Interestingly, the changes induced by BR were less pronounced in the HMB group.

RNA-seq also revealed marked reduction of transcripts associated with mitochondria and mitochondrial energy metabolic pathways (Supplementary Figures 2 and 3). These included the mitochondrial inner membrane and oxidative phosphorylation. Given the marked inhibition of pathways associated with mitochondrial energy metabolism, we further examined the RNA-seq data for changes in mitochondrial energy metabolic genes. Transcripts encoding proteins in fatty acid degradation, TCA cycle, and the electron transport chain were comprehensively down-regulated (Figure 3A, Supplementary Tables 4 and 5). Moreover, using upstream regulator analysis, genes controlling mitochondrial biogenesis and energy metabolism such

Table 1. Subject Characteristics

	Control		HMB		2 × 2 ANOVA (*p* value)		
Subject Characteristics	**Pre**	**Post**	**Pre**	**Post**	**Group**	**Time**	**Interaction**
N (M/F)	9 (6/3)		12 (5/7)				
Age (years)	67 ± 2		66 ± 1		0.21	0.88	0.88
Height (cm)	170.9 ± 2.4		162.8 ± 3.6		**0.02**	0.95	0.95
Weight (kg)	77.7 ± 5.1	76.1 ± 5.4	81.7 ± 3.9	79.8 ± 4.0	0.41	0.71	0.98
BMI (kg/m^2)	26.4 ± 1.4	25.7 ± 1.4	30.8 ± 0.9	30.0 ± 0.9	**0.001**	0.54	0.98

Note: Data are mean ± SE. Bold *p* values indicate statistical significance ($p < .05$). ANOVA = Analysis of variance; BMI = Body mass index; HMB = β-hydroxy-β-methylbutyrate.

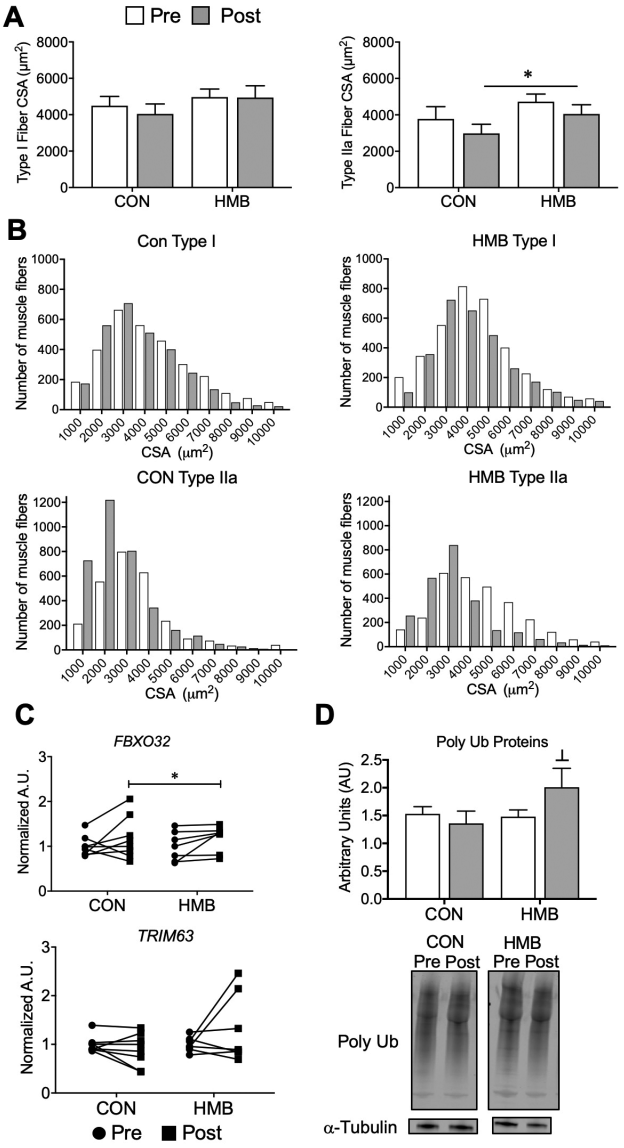

Figure 1. Older adults display reductions in type IIa skeletal muscle fiber cross-sectional area (CSA) and elevations in skeletal muscle markers of atrophy following 10 days of bed rest (BR). (**A**) Type I and type IIa, and (**B**) frequency histograms of skeletal muscle fiber CSA depicting sampled vastus lateralis muscle fibers pre- and post-10 days of BR; $n = 9–12$ per group. † main effect for time for both groups: Type IIa CSA (Time Effect: $p = .03$, Interaction: $p = .85$). (**C**) Gene expression of atrophy markers and (**D**) western blot and representative images pre- and post-10 days BR. Vertical dividing lines were used in Western blot images to present lanes from the same gel that were reorganized for presentation purpose; $n = 5–9$ per group. † trend for main effect for time for both groups: atrogin-1 (Time Effect: $p = .069$, Interaction: $p = .97$); ⊥ Trend for a group effect from pre-BR: poly-ubiquinated proteins (Group Effect: $p = .078$, Interaction: 0.10).

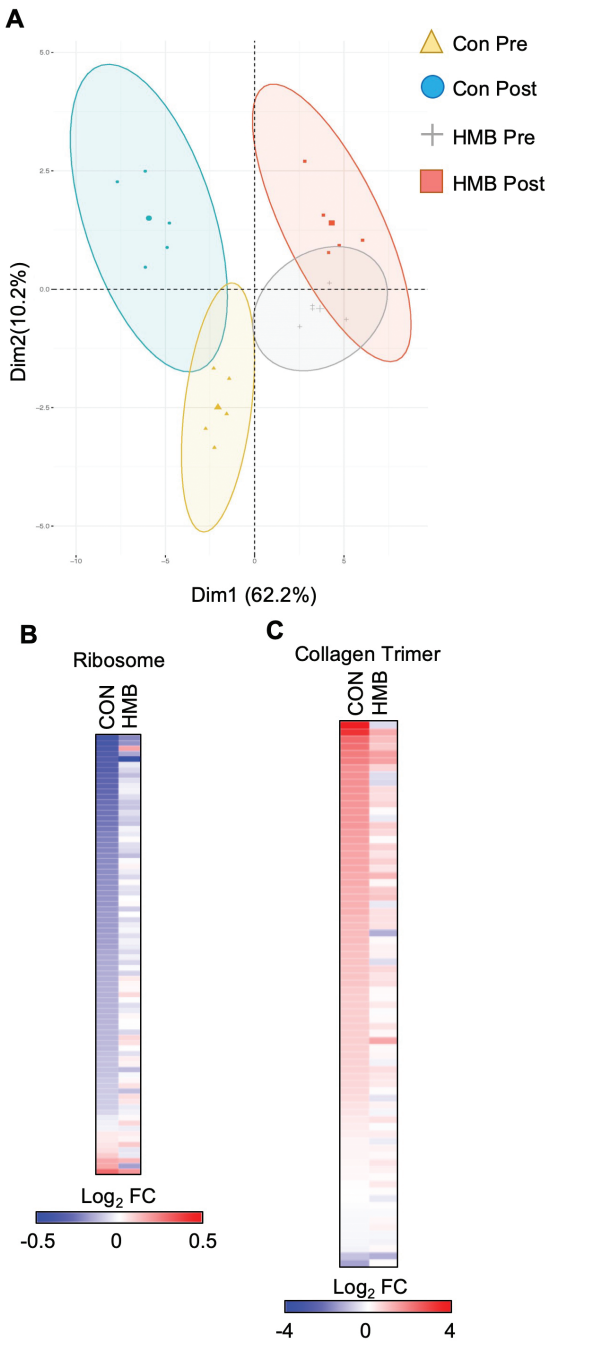

Figure 2. Bed rest (BR) results in a marked inhibition of skeletal muscle metabolism, ribosome, and collagen pathways. (**A**) Principal component analysis plot of the samples used in the transcriptomic analysis. (**B**) The heat map represents the $\log_2$ fold change of all transcripts in the KEGG Ribosome pathway during BR in either the CON or β-hydroxy-β-methylbuturate (HMB) group. (**C**) The heat map represents the $\log_2$ fold change of all transcripts in the GO CC Collagen Trimer pathway during BR in either the CON or HMB group. $n = 5$ per group for transcriptomic analysis. Full color version is available within the online issue.

as PGC1-α (*PPARGC1A*), ERRα (*ESRRA*), and PPARα (*PPARA*) were all predicted to be inhibited (Figure 3B). The expression of both PGC-1α and ERRα as well as direct target genes as determined by RT-qPCR were down-regulated with BR (Figure 3C). These data suggest that direct down-regulation of these key transcriptional regulators is, at least in part, responsible for the inhibition of mitochondrial energy metabolic pathways.

HMB supplementation markedly blunted the muscle transcriptomic responses to BR. This is particularly evident in the pathway analysis in which the degree of changes on the indicated pathways was diminished in the HMB (Supplementary Figures 2 and 3). The targeted gene expression analyses confirmed these unbiased transcriptomic profiling; although there is still a decrease in the expression of mitochondrial energy metabolic genes, the number of genes and degree of change is smaller in the HMB group (Figure 3A).

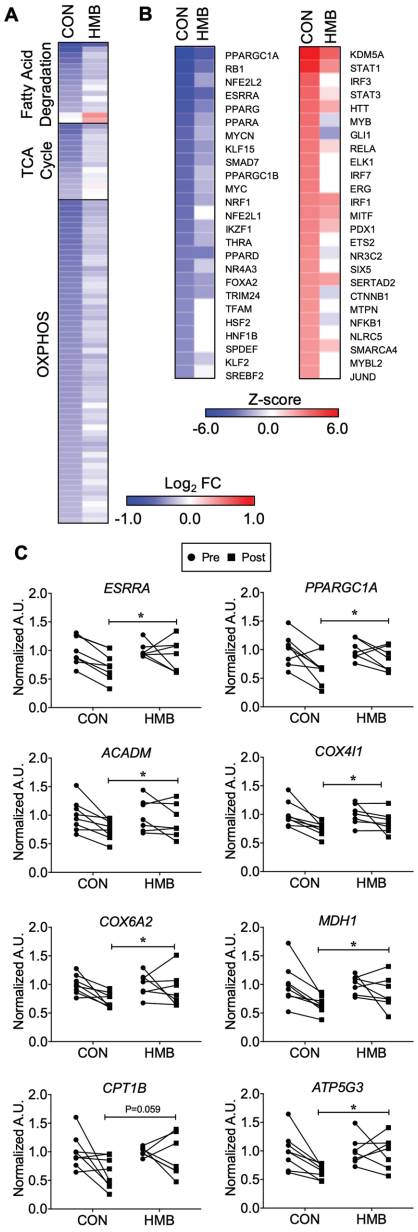

Figure 3. Gene regulatory networks involved in skeletal muscle oxidative metabolism are down-regulated following 10 days of bed rest (BR). (**A**)The heat map represents the $\log_2$ fold change of all transcripts in the indicated KEGG pathway that are significantly regulated ($p < .05$) during BR in either the CON or β-hydroxy-β-methylbuturate (HMB) groups. (**B**) IPA Upstream Regulator Analysis was used to identify transcription regulators and ligand activated transcription factors significantly regulated (Z-score >2 or <–2) in either CON or HMB groups. The heat map represents the Z-score for the top 25 inhibited (left) or activated (right) factors in the CON group and the corresponding Z-score in the HMB group. $n = 5$ per group for transcriptomic analysis. OXPHOS = oxidative phosphorylation. (**C**) RT-qPCR assay for expression of key nuclear transcription factors, and genes involved in fuel metabolism pre- and post- 10 days of BR. $n = 7$–8 per group. * Significant time effect for reductions following BR: ERRα (*ESRRA*) (Time Effect: $p = .01$, Interaction: $p = .19$), PGC1-α (*PPARGC1A*) (Time Effect: $p = .003$, Interaction: $p = .25$), MCAD (*ACADM*) (Time Effect: $p = .001$, Interaction: $p = .19$), COX4I1 (*COX4I1*) (Time Effect: $p = .002$, Interaction: $p = .30$), COX6A2 (*COX6A2*) (Time Effect: $p = .03$, Interaction: $p = .23$), ATP synthase (*ATP5G3*) (Time Effect: $p = .03$, Interaction: $p = .06$) and MDH1 (*MDH1*) (Time Effect: $p = .005$, Interaction: $p = .19$). † trend for time effect for CPT1 (CPT1B) (Time Effect: $p = .058$, Interaction: $p = .20$) to be reduced following BR. Full color version is available within the online issue.

Skeletal Muscle Mitochondrial Function and Content, and H_2O_2 Emission

Skeletal muscle mitochondrial respiration and content, and H_2O_2 emission are presented in Figure 4A–C. The HMB group had a slightly lower, but significant, LI respiration before BR compared to CON (Group Effect: $p = .008$, Interaction: $p = .44$; Figure 4A). There was a significant time effect for PI (Time Effect: $p = .03$, Interaction: 0.91) and EI+II (Time Effect: $p = .01$, Interaction: $p = .96$), and trend for PI+II (Time Effect: $p = .059$, Interaction: $p = .71$) to be reduced in both groups following BR (Figure 4A). Mitochondrial H_2O_2 emission tended to increase in both groups following BR (Time Effect $p = .056$, Interaction: $p = .61$; Figure 4B). Total mitochondrial OXPHOS content (Time Effect: $p = .002$, Interaction: $p = .34$) and all individual complexes: complex I (Time Effect: $p = .005$, Interaction: $p = .31$), complex II (Time Effect: $p = .008$, Interaction: $p = .32$), complex III (Time Effect: $p = .004$, Interaction: $p = .28$), complex IV (Time Effect: $p = .017$, Interaction: $p = .76$) and complex V (Time Effect: $p = .03$, Interaction: $p = .64$), were reduced in both groups following BR (Figure 4C).

Skeletal Muscle Lipidomics

Lipidomics analysis was next performed to measure changes of lipids critical to mitochondrial energy metabolism. Total levels of cardiolipin, the major phospholipid component in mitochondrial membranes, are significantly decreased with BR (Time Effect: $p = .04$, Interaction: $p = .42$) while levels of the ETC component coenzyme Q10 (Time Effect: $p = .0577$, Interaction: $p = .92$) tended to decrease following BR (Figure 4D). Cardiolipin species can be categorized based on acyl chain length and degree of saturation, into: immature, mature, and remodeled species (28). The heat map and table of individual species show reduced levels of virtually all cardiolipin species in the CON group and a slight preservation effect of HMB following BR (Figure 4D, Supplementary Table 6). There were no significant changes in total phosphatidylcholine (PC), phosphatidylethanolamine (PE), PC:PE ratio, sphingomyelin, triacylglycerol (TAG), diacylglycerol, ceramides, and acylcarnitines following BR ($p > .05$, Supplementary Figure 4).

Discussion

The effect of short-term BR on skeletal muscle mitochondria has not been studied in older adults, and only a few studies have examined mitochondrial adaptation to BR in young healthy volunteers (11,16,18,29). The goal of this investigation was to examine mitochondrial energetics in human skeletal muscle following 10 days of BR in older adults, using a combination of targeted and unbiased approaches. The principal novel findings were that BR induced a significant decrease in mitochondrial respiration and content, and elevated mitochondrial reactive oxygen species (ROS) emission. These findings were supported by unbiased transcriptomic profiling that revealed down-regulation of transcripts involved in skeletal muscle ribosome and fuel metabolism pathways (fatty acid degradation, TCA cycle, OXPHOS), along with up-regulation of transcripts involved in collagen synthesis.

Utilizing unbiased transcriptomics, we identified down- and up-regulated GO cellular components and KEGG pathways that were impacted by 10 days of BR that likely have implications for skeletal muscle health. We found a significant down regulation of skeletal muscle oxidative metabolism and mitochondria, and HMB mitigated this response. These findings are supported by our recent

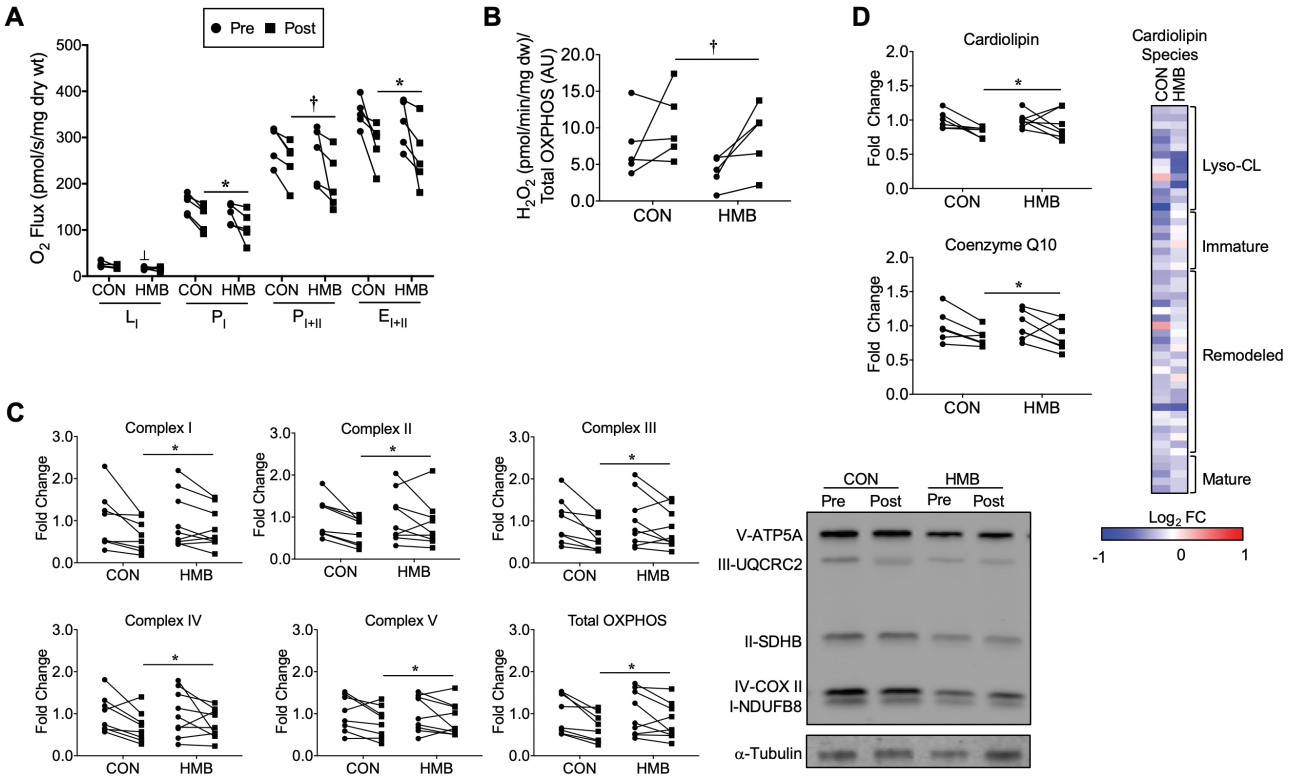

Figure 4. Skeletal muscle mitochondrial function, OXPHOS, cardiolipin, and coenzyme Q10 content are reduced, and H_2O_2 emission is elevated following 10 days of BR. (**A**) Mitochondrial respiratory capacity was measured in permeabilized fiber bundles and reported as O_2 flux normalized to the dry weight of the fiber bundles; $n = 5$ per group. (**B**) Mitochondrial H_2O_2 emission was measured in permeabilized fiber bundles and reported as H_2O_2 emission normalized to total OXPHOS content; $n = 5$ per group. (**C**) Skeletal muscle mitochondria oxidative phosphorylation (OXPHOS) content pre- and post-10 days of BR and representative Western blot images; $n = 8$–9 per group. Pre- and post-BR data are reported as fold change from pre-BR. (**D**) Skeletal muscle total cardiolipin and coenzyme Q10 pre- and post-10 days of BR; $n = 6$–7 per group. ⊥ Significant group effect for HMB group pre-BR (Group Effect: $p = .008$, Interaction: $p = .44$), * Significant time effect for PI (Time Effect: $p = .03$, Interaction: 0.91) and EI+II (Time Effect: $p = .01$, Interaction: $p = .96$) to be reduced in both groups following BR, and † trend for time effect for PI+II (Time Effect: $p = .059$, Interaction: $p = .71$) to be reduced in both groups following BR. † trend for time effect for H_2O_2 emission to be elevated in both groups following 10 days of BR (Time Effect $p = .056$, Interaction: $p = .61$). * Significant time effect for reductions in both groups for total OXPHOS content (Time Effect: $p = .002$, Interaction: $p = .34$), complex I (Time Effect: $p = .005$, Interaction: $p = .31$), complex II (Time Effect: $p = .008$, Interaction: $p = .32$), complex III (Time Effect: $p = .004$, Interaction: $p = .28$), complex IV (Time Effect: $p = .017$, Interaction: $p = .76$) and complex V (Time Effect: $p = .03$, Interaction: $p = .64$). * Significant time effect for cardiolipin (Time Effect: $p = .04$, Interaction: 0.42) and † trend for time effect for coenzyme Q10 (Time Effect: $p = .0577$, Interaction: $p = .92$) to be reduced following BR. The heat map represents the $\log_2$ fold change of all cardiolipin species during BR in the CON and HMB groups. The cardiolipin species are grouped according to the maturation status of each species. $n = 5$ per group. Red (up-regulated) and blue (down regulated) dots represent significantly changed metabolites during BR. Full color version is available within the online issue.

findings in a preclinical animal model of disuse atrophy in which several upstream regulators, for example, PGC-1α and ERRα, of mitochondrial biogenesis and energetics were significantly affected (30). Mahmassani et al. also found mitochondrial dysfunction and oxidative phosphorylation pathways were significantly regulated in both young and old individuals following 5 days of BR (31). Collectively, these studies highlight the potent effect of short-term disuse on skeletal muscle oxidative metabolism and mitochondrial transcriptome.

Down-regulation of transcripts associated with skeletal muscle metabolism and mitochondria were concomitant with an impact on ex vivo mitochondrial respiration, markers of content, and ROS emission. The reductions in mitochondrial respiration with BR in these older subjects are consistent with studies in younger adults (17) as well as in our recent findings in older mice following 10 days of hindlimb (HL) unloading (30). The reductions in mitochondrial respiration following BR could have significant ramifications for older adults during disuse atrophy and also when they become ambulatory during recovery from illness or injury. Several studies have found that lower mitochondrial oxidative capacity and efficiency are associated with lower muscle quality (32), slower walking speed (33,34), and higher fatigability (35). Collectively, our study, supported by these previous findings, suggests that reductions in mitochondrial function during a short period of disuse may be associated with a reduction in physical function of older adults. The reductions in mitochondrial respiration were likely driven by the reductions in mitochondrial content (OXPHOS proteins and cardiolipin). Other investigations have described reductions in mitochondrial content following 7 days BR in young men (16) and 10 days of HL unloading in mice (30). Indeed, the reduction in total cardiolipin content, respiration, and expression of mitochondrial biogenic transcription factors together demonstrate a profound reduction in mitochondrial content and function following BR.

Mitochondrial dysfunction during inactivity or immobilization manifests through the release of proapoptotic factors (36,37), morphological alterations (fission, swelling), and energy stress (9) leading to ROS production. ROS stimulates muscle atrophy by increasing proteins involved in the proteasome system (38). We found older adults had higher ROS emission with no significant changes in skeletal

muscle lipids following 10 days of BR (Figures 4B and Supplementary Figure 4). Dirks et al. found no changes in markers of oxidative stress and skeletal muscle lipids following 7 days BR in young men (16). Collectively, these findings suggest that younger individuals may not be as susceptible as older adults to disuse induced oxidative stress. Indeed, upon reloading after 10 days of HL unloading, older mice still had elevated ROS emission while the ROS emission in younger mice returned to baseline (30). Older muscle may be more susceptible to disuse induced ROS emission compared to younger adults and may persist into recovery. These are similar findings to our previous investigation after 10 days of BR in older adults (18) and in young individuals (16). Further investigations could focus on earlier time points during BR to assess temporal sequence of changes that occur in mitochondria and with the transcriptome prior to significant muscle atrophy. Finally, although we previously reported an increase in TAG levels in older adults consuming HMB during BR (18); in the current investigation, we did not see any significant changes in TAG with BR or HMB supplementation.

Although no effect on skeletal muscle fiber CSA was observed, HMB supplementation abrogated many of the transcriptomic changes during BR. This was particularly apparent with transcripts associated with mitochondrial energy metabolism, ribosome, and extracellular matrix. In spite of the effects on the mitochondrial transcripts, respiration rates did not significantly differ between CON and HMB, suggesting other mechanisms such as posttranslational modifications may also contribute to the mitochondrial dysfunction observed with BR. The observation that HMB counteracted the effect of BR on the ribosome transcripts is consistent with its effects to stimulate protein synthesis (39–41). Lastly, we found the extracellular matrix and collagen pathways to be significantly up-regulated in the CON group with BR, which was attenuated in the HMB group. A recent investigation also found fibrotic pathways to be significantly up-regulated in older adults after 5 days of BR (31). Up-regulation of the extracellular matrix and collagen proteins may have important implications for skeletal muscle function. Rats who were HL unloaded for 14 and 28 days had collagen remodeling that resulted in muscle stiffness, which can impact muscle fatigability (42). Taken together, these findings suggest that HMB has a major impact on skeletal muscle at the gene transcript level, which may prove beneficial for the recovery following short-term disuse. A previous study has shown older adults receiving HMB supplementation during an 8-week exercise recovery program following 10 days of BR resulted in additional muscle mass and strength gains compared to a control group (43). Combining HMB with an exercise regimen following a period of disuse or hospitalization may have significant impact on clinical outcomes in sedentary older adults. Collectively, these data have important clinical implications as muscle mass and function are impacted not only in natural aging but also conditions such as sarcopenia and cancer cachexia. Future investigations are needed to explore the effect of HMB supplementation combined with exercise in these clinical populations.

The goal of the present study was to take an unbiased and in-depth approach to understanding the effects of BR on skeletal muscle metabolism, so we did not perform a biopsy following recovery from BR. This limits our interpretation of the effects of HMB's effect on skeletal muscle recovery. Additionally, comparing these effects between older adults and younger subjects was also not our objective. Moreover, while men have higher muscle mass and strength than women, we observed no trends for gender-specific responses, and our study was not designed or powered to determine gender differences. During BR, subjects underwent passive range of motion exercises to help prevent DVT. While there is evidence that stretching may activate mechanotransduction signaling pathways, we do not believe the passive exercises would impact our results as they were conducted one time a day lasting ~10 minutes. We acknowledge the small number of subjects in this study and the subsequent impact of smaller sample sizes for some of the analyses limits our interpretation of our findings. Additional studies are needed to confirm the findings presented in this study.

In summary, our data implicate derangements in skeletal muscle metabolism and mitochondria during BR-induced muscle atrophy in older adults. HMB significantly attenuated or prevented some of the negative consequences of disuse on expression of skeletal muscle genes involved in mitochondrial biogenesis and energetics, fatty acid metabolism, ribosome pathways (protein synthesis), and collagen accumulation. Future investigations are needed to determine whether these effects are important for better recovery of muscle mass and function following periods of disuse.

Supplementary Material

Supplementary data is available at *The Journals of Gerontology, Series A: Biological Sciences and Medical Sciences* online.

Supplemental Figure 1. Representative histology images for both CON and HMB groups at pre-BR and post-BR.

Supplemental Figure 2. Gene ontology enrichment analysis using DAVID. (A) All significantly ($p < .05$) down regulated transcripts during BR in the CON and HMB groups. (B) All significantly ($p < .05$) up regulated transcripts during BR in the CON and HMB groups. The bars represent -log (p-value) of the top 10 most significant gene ontology cellular component terms in each group; $n = 5$ per group.

Supplemental Figure 3. Pathway enrichment analysis using DAVID. (A) All significantly ($p < .05$) down regulated transcripts during BR in the CON and HMB groups. (B) All significantly ($p < .05$) up regulated transcripts during BR in the CON and HMB groups. The bars represent -log (p-value) of the top 10 most significant KEGG terms in each group; $n = 5$ per group.

Supplemental Figure 4. Skeletal muscle lipids following 10 days of BR in the CON and HMB groups. Phosphatidylcholine (PC), phosphatidylethanolamine (PE), PC:PE ratio, sphingomyelin (SM), triacylglycerol (TAG), diacylglycerol (DAG), ceramides, and acylcarnitines (AC). $n = 6–7$ per group.

Funding

This work was supported by Abbott Nutrition, Abbott Laboratories

Acknowledgments

The authors gratefully appreciate the contributions of our study participants. Author Contributions: P.M.C. and B.H.G. contributed by designing and overseeing the clinical study. R.A.S., G.D., M.B.T., and R.B.V. were involved in conducting the experiments, acquiring, and analyzing the data. D.P.K. provided support and reagents for sample analysis. E.C., N.R.N., B.G., G.K., V.V.T., and M.A.K. contributed by generating and analyzing the metabolomics and lipisomics data. G.Y., R.B.V., and F.Q. provided bioinformatics support. R.A.S. wrote the manuscript. R.A.S., P.M.C., and R.B.V. edited the manuscript.

Conflict of Interest

P.M.C. is a consultant for Astellas/Mitobridge, Inc; D.P.K. is a consultant for Pfizer, Amgen, and Janssen.

References

1. Gibson JN, Halliday D, Morrison WL, et al. Decrease in human quadriceps muscle protein turnover consequent upon leg immobilization. *Clin Sci (Lond)*. 1987;72:503–509. doi: 10.1042/cs0720503
2. DeFrances CJ, Lucas CA, Buie VC, Golosinskiy A. National hospital discharge survey. *Natl Health Stat Report*. 2006;2008:1–20. https://www.cdc.gov/nchs/data/nhsr/nhsr005.pdf
3. Kortebein P, Ferrando A, Lombeida J, Wolfe R, Evans WJ. Effect of 10 days of bed rest on skeletal muscle in healthy older adults. *JAMA*. 2007;297:1772–1774. doi: 10.1001/jama.297.16.1772-b
4. Suetta C, Frandsen U, Mackey AL, et al. Ageing is associated with diminished muscle re-growth and myogenic precursor cell expansion early after immobility-induced atrophy in human skeletal muscle. *J Physiol*. 2013;591:3789–3804. doi: 10.1113/jphysiol.2013.257121
5. Coker RH, Hays NP, Williams RH, Wolfe RR, Evans WJ. Bed rest promotes reductions in walking speed, functional parameters, and aerobic fitness in older, healthy adults. *J Gerontol A Biol Sci Med Sci*. 2015;70:91–96. doi: 10.1093/gerona/glu123
6. Fortinsky RH, Covinsky KE, Palmer RM, Landefeld CS. Effects of functional status changes before and during hospitalization on nursing home admission of older adults. *J Gerontol A Biol Sci Med Sci*. 1999;54:M521–M526. doi: 10.1093/gerona/54.10.m521
7. Mithal A, Bonjour JP, Boonen S, et al.; IOF CSA Nutrition Working Group. Impact of nutrition on muscle mass, strength, and performance in older adults. *Osteoporos Int*. 2013;24:1555–1566. doi: 10.1007/s00198-012-2236-y
8. Smuder AJ, Kavazis AN, Hudson MB, Nelson WB, Powers SK. Oxidation enhances myofibrillar protein degradation via calpain and caspase-3. *Free Radic Biol Med*. 2010;49:1152–1160. doi: 10.1016/j.freeradbiomed.2010.06.025
9. Romanello V, Guadagnin E, Gomes L, et al. Mitochondrial fission and remodelling contributes to muscle atrophy. *EMBO J*. 2010;29:1774–1785. doi: 10.1038/emboj.2010.60
10. Cannavino J, Brocca L, Sandri M, Bottinelli R, Pellegrino MA. PGC1-alpha over-expression prevents metabolic alterations and soleus muscle atrophy in hindlimb unloaded mice. *J Physiol*. 2014;592:4575–4589. doi:10.1113/jphysiol.2014.275545
11. Coker RH, Hays NP, Williams RH, Xu L, Wolfe RR, Evans WJ. Bed rest worsens impairments in fat and glucose metabolism in older, overweight adults. *J Gerontol A Biol Sci Med Sci*. 2014;69:363–370. doi: 10.1093/gerona/glt100
12. Bergouignan A, Rudwill F, Simon C, Blanc S. Physical inactivity as the culprit of metabolic inflexibility: evidence from bed-rest studies. *J Appl Physiol (1985)*. 2011;111:1201–1210. doi: 10.1152/japplphysiol.00698.2011
13. Cree MG, Paddon-Jones D, Newcomer BR, et al. Twenty-eight-day bed rest with hypercortisolemia induces peripheral insulin resistance and increases intramuscular triglycerides. *Metabolism*. 2010;59:703–710. doi: 10.1016/j.metabol.2009.09.014
14. Paddon-Jones D, Sheffield-Moore M, Cree MG, et al. Atrophy and impaired muscle protein synthesis during prolonged inactivity and stress. *J Clin Endocrinol Metab*. 2006;91:4836–4841. doi: 10.1210/jc.2006-0651
15. Goodpaster BH. Mitochondrial deficiency is associated with insulin resistance. *Diabetes*. 2013;62:1032–1035. doi: 10.2337/db12-1612
16. Dirks ML, Wall BT, van de Valk B, et al. One week of bed rest leads to substantial muscle atrophy and induces whole-body insulin resistance in the absence of skeletal muscle lipid accumulation. *Diabetes*. 2016;65:2862–2875. doi: 10.2337/db15-1661
17. Kenny HC, Rudwill F, Breen L, et al. Bed rest and resistive vibration exercise unveil novel links between skeletal muscle mitochondrial function and insulin resistance. *Diabetologia*. 2017;60:1491–1501. doi: 10.1007/s00125-017-4298-z
18. Standley RA, Distefano G, Pereira SL, et al. Effects of beta-hydroxy-beta-methylbutyrate (HMB) on skeletal muscle mitochondrial content and dynamics, and lipids after 10 days of bed rest in older adults. *J Appl Physiol (1985)*. 2017;123:1092–1100. doi:10.1152/japplphysiol.00192.2017
19. He X, Duan Y, Yao K, Li F, Hou Y, Wu G, et al. beta-Hydroxy-beta-methylbutyrate, mitochondrial biogenesis, and skeletal muscle health. *Amino Acids*. 2016;48:653–664. doi:10.1007/s00726-015-2126-7
20. Pinheiro CH, Gerlinger-Romero F, Guimarães-Ferreira L, et al. Metabolic and functional effects of beta-hydroxy-beta-methylbutyrate (HMB) supplementation in skeletal muscle. *Eur J Appl Physiol*. 2012;112:2531–2537. doi: 10.1007/s00421-011-2224-5
21. Pruchnic R, Katsiaras A, He J, Kelley DE, Winters C, Goodpaster BH. Exercise training increases intramyocellular lipid and oxidative capacity in older adults. *Am J Physiol Endocrinol Metab*. 2004;287:E857–E862. doi: 10.1152/ajpendo.00459.2003
22. Coen PM, Menshikova EV, Distefano G, et al. Exercise and weight loss improve muscle mitochondrial respiration, lipid partitioning, and insulin sensitivity after gastric bypass surgery. *Diabetes*. 2015;64:3737–3750. doi: 10.2337/db15-0809
23. Anderson EJ, Lustig ME, Boyle KE, et al. Mitochondrial H2O2 emission and cellular redox state link excess fat intake to insulin resistance in both rodents and humans. *J Clin Invest*. 2009;119:573–581. doi: 10.1172/JCI37048
24. Behan WM, Cossar DW, Madden HA, McKay IC. Validation of a simple, rapid, and economical technique for distinguishing type 1 and 2 fibres in fixed and frozen skeletal muscle. *J Clin Pathol*. 2002;55:375–380. doi: 10.1136/jcp.55.5.375
25. Brocca L, Cannavino J, Coletto L, et al. The time course of the adaptations of human muscle proteome to bed rest and the underlying mechanisms. *J Physiol*. 2012;590:5211–5230. doi: 10.1113/jphysiol.2012.240267
26. Kiebish MA, Bell R, Yang K, et al. Dynamic simulation of cardiolipin remodeling: greasing the wheels for an interpretative approach to lipidomics. *J Lipid Res*. 2010;51:2153–2170. doi: 10.1194/jlr.M004796
27. Simons B, Kauhanen D, Sylvänne T, Tarasov K, Duchoslav E, Ekroos K. Shotgun lipidomics by sequential precursor ion fragmentation on a hybrid quadrupole time-of-flight mass spectrometer. *Metabolites*. 2012;2:195–213. doi: 10.3390/metabo2010195
28. Pennington ER, Funai K, Brown DA, Shaikh SR. The role of cardiolipin concentration and acyl chain composition on mitochondrial inner membrane molecular organization and function. *Biochim Biophys Acta Mol Cell Biol Lipids*. 2019;1864:1039–1052. doi: 10.1016/j.bbalip.2019.03.012
29. Pišot R, Marusic U, Biolo G, et al. Greater loss in muscle mass and function but smaller metabolic alterations in older compared with younger men following 2 wk of bed rest and recovery. *J Appl Physiol (1985)*. 2016;120:922–929. doi: 10.1152/japplphysiol.00858.2015
30. Zhang X, Trevino MB, Wang M, et al. Impaired mitochondrial energetics characterize poor early recovery of muscle mass following hind limb unloading in old mice. *J Gerontol A Biol Sci Med Sci*. 2018;73:1313–1322. doi: 10.1093/gerona/gly051
31. Mahmassani ZS, Reidy PT, McKenzie AI, Stubben C, Howard MT, Drummond MJ. Age-dependent skeletal muscle transcriptome response to bed rest-induced atrophy. *J Appl Physiol (1985)*. 2019;126:894–902. doi:10.1152/japplphysiol.00811.2018
32. Distefano G, Standley RA, Zhang X, et al. Physical activity unveils the relationship between mitochondrial energetics, muscle quality, and physical function in older adults. *J Cachexia Sarcopenia Muscle*. 2018;9:279–294. doi: 10.1002/jcsm.12272
33. Coen PM, Jubrias SA, Distefano G, et al. Skeletal muscle mitochondrial energetics are associated with maximal aerobic capacity and walking speed in older adults. *J Gerontol A Biol Sci Med Sci*. 2013;68:447–455. doi: 10.1093/gerona/gls196
34. Zane AC, Reiter DA, Shardell M, et al. Muscle strength mediates the relationship between mitochondrial energetics and walking performance. *Aging Cell*. 2017;16:461–468. doi: 10.1111/acel.12568
35. Santanasto AJ, Glynn NW, Jubrias SA, et al. Skeletal muscle mitochondrial function and fatigability in older adults. *J Gerontol A Biol Sci Med Sci*. 2015;70:1379–1385. doi: 10.1093/gerona/glu134
36. Adhihetty PJ, O'Leary MF, Chabi B, Wicks KL, Hood DA. Effect of denervation on mitochondrially mediated apoptosis in

skeletal muscle. *J Appl Physiol (1985)*. 2007;102:1143–1151. doi: 10.1152/japplphysiol.00768.2006

37. Max SR. Disuse atrophy of skeletal muscle: loss of functional activity of mitochondria. *Biochem Biophys Res Commun*. 1972;46:1394–1398. doi: 10.1016/s0006-291x(72)80130-x
38. Reid MB. Response of the ubiquitin-proteasome pathway to changes in muscle activity. *Am J Physiol Regul Integr Comp Physiol*. 2005;288:R1423–R1431. doi: 10.1152/ajpregu.00545.2004
39. Wilkinson DJ, Hossain T, Hill DS, Phillips BE, Crossland H, Williams J, et al. Effects of leucine and its metabolite beta-hydroxy-beta-methylbutyrate on human skeletal muscle protein metabolism. *J Physiol*. 2013;591:2911–2923. doi:10.1113/jphysiol.2013.253203
40. Girón MD, Vílchez JD, Salto R, et al. Conversion of leucine to β-hydroxy-β-methylbutyrate by α-keto isocaproate dioxygenase is required for a potent stimulation of protein synthesis in L6 rat myotubes. *J Cachexia Sarcopenia Muscle*. 2016;7:68–78. doi: 10.1002/jcsm.12032
41. Wheatley SM, El-Kadi SW, Suryawan A, et al. Protein synthesis in skeletal muscle of neonatal pigs is enhanced by administration of beta-hydroxy-beta-methylbutyrate. *Am J Physiol Endocrinol Metab*. 2014;306:E91–99. doi:10.1152/ajpendo.00500.2013
42. Miller TA, Lesniewski LA, Muller-Delp JM, Majors AK, Scalise D, Delp MD. Hindlimb unloading induces a collagen isoform shift in the soleus muscle of the rat. *Am J Physiol Regul Integr Comp Physiol*. 2001;281:R1710–R1717. doi: 10.1152/ajpregu.2001.281.5.R1710
43. Deutz NE, Pereira SL, Hays NP, et al. Effect of beta-hydroxy-beta-methylbutyrate (HMB) on lean body mass during 10 days of bed rest in older adults. *Clinical nutrition*. 2013;32:704–712. doi:10.1016/j.clnu.2013.02.011